Boundary Layer Lubrication: Tribofilms and Subsurface Deformation Mechanisms

[1]J. Hershberger,[1] O. O. Ajayi
[1]Argonne National Laboratory, Argonne, IL, U.S.A.

Introduction

Boundary layer lubrication is the most severe regime of wear before the occurrence of catastrophic failure in the form of scuffing. Scuffing is characterized by a sudden rise in friction, surface roughening, heating, and, sometimes, material transfer and/or welding. Formulated oils, such as automotive engine lubricants, contain additives whose functions include enhancing extreme-pressure performance. These additives work by forming a protective solid film ("tribofilm") on the rubbing surfaces through chemical reactions, which are assisted by the elevated temperatures at asperities. Surface treatments such as carburization, nitriding, and coating are also used to enhance scuffing resistance.

Past investigations into scuffing have generally been performed by varying wear test conditions, constructing a map of scuffing failure zones, and using the map to formulate a rule of thumb for design purposes. Several theories on the initiation of scuffing have been proposed, and each theory or rule of thumb accounts for only a limited subset of the data. Apart from the mechanical test itself and optical or scanning electron microscopy of the failed surfaces, few analytical methods have been applied to the problem. As a result, understanding of the fundamental mechanisms of scuffing is limited [1, 2].

The lubricant design community also employs an empirical approach. It relies on several decades of knowledge about the effects of additives and their interactions with materials, base stocks, and one another. However, in the next several years, emission regulations are projected to become restrictive enough that the contribution of engine lubricants to tailpipe emissions will have to be reduced. A new generation of additives will be needed to minimize S, P, and heavy metal content. The experience-based methods used to date are not equipped to meet this need in the time scale desired. The oil environment of the tribofilms presents an added complication, in that oil is incompatible with many analytical methods (such as x-ray photoelectron spectroscopy, auger spectroscopy, and transmission electron microscopy), and rinsing off the oil with solvents changes the structure of the tribofilm [3].

Clearly, analytical techniques are needed to provide information on the structure and composition of the tribofilms and the deformation mechanisms operating beneath the surface. The approach taken in this project has been to use x-rays as a probe, collecting information from the surface films and the subsurface in separate experiments. The tribofilms are interrogated, without rinsing off the oil, by means of x-ray fluorescence (XRF) and x-ray diffraction (XRD) in the grazing incidence mode and by x-ray reflectivity (XRR). Scuffing initiation mechanisms are investigated by analysis of grazing-incidence-XRD peak broadening in unworn, partially scuffed, and scuffed metal samples.

We have developed a theory relating the initiation of scuffing to subsurface deformation mechanisms. This theory states that scuffing occurs by adiabatic shear instability, when work hardening is balanced by thermal softening. The scuffing resistance of a material is predicted from the parameter γ, calculated from microstructural parameters as:

$$\gamma = \frac{n\rho C_v}{0.9\frac{\partial \tau}{\partial T}} \ ,$$

where γ = shear strain, n = the work hardening index, ρ = density, C_v = specific heat capacity, and τ = shear strength. This prediction is being checked against the mechanical results and the dislocation density as measured from XRD peak broadening.

Methods and Materials

Tribofilm samples were prepared both thermally and thermomechanically from model-formulated oils consisting of polyalphaolefin (PAO) base oil and 1.5 wt% additive. The additives used were zinc alkyl dithiophosphate, molybdenum di(2-ethylexyl)phosphorodithioate, tricresyl phosphate, chloroform, and dimethyl disulfide. The tribofilms were formed on flats of H-13 steel polished to a roughness of 10-20 Å as measured by atomic force microscopy (AFM) and XRR. The thermal films were made by submerging the flats in the oils and heating to 150ºC for 24 h. Thermomechanical films were formed in a hot wear test, in which the side of a 1.3-m-long, 0.9-cm-diameter Delrin polymer cylinder was rubbed against a flat, lubricated by an oil, at 70ºC for 5 h. This low-severity wear was chosen to minimize mechanical roughening of the polished flat.

The block samples for the block-on-ring wear tests were made of SAE 4340 steel. The samples were cut to shape, austenitized and quenched, and then tempered for 1 h. Each of the five sample groups was tempered at a

different temperature, as listed in Table 1. The hardnesses, scuffing loads, and values of the microstructural parameter γ after tempering are also listed in Table 1.

Table 1. Tempering temperature, hardness, gamma, and scuffing load for samples of Group 1 through 5.

Group	Tempering Temp. (°C)	Hardness, *(R)*	γ	Scuffing Load (lb)
1	204	53	0.1	22.0
2	260	50	0.086	22.8
3	316	46	0.094	21.8
4	540	39	0.245	19.5

The scuffing tests were performed in a Falex block-on-ring wear tester by using a lubricant of PAO base stock whose kinematic viscosity was 18 cSt at 40°C. Contact severity was increased by using the step-load increase protocol, at a loading rate of 8.9 N (2 lb) per 1-min step. Friction was monitored during the test, and the test machine was stopped immediately after the occurrence of scuffing, as defined by a rise in friction to a value over 0.3.

The x-ray experiments were performed at beamline 12-BM at the APS, a bending magnet station operated by the Basic Energy Sciences Synchrotron Radiation Center Collaborative Access Team (BESSRC-CAT). A photon energy of 20 keV was selected, and a Ge(111) monochromator crystal was used to define the 2θ resolution.

Results

XRR and depth-profiled XRD experiments were performed on 18 tribofilm samples. XRR data were compared to simulations that modeled the system as a steel substrate, a layer of iron oxide, a layer of tribofilm, and an ambient medium of oil. The method of simulation was derived from Parratt [4]. Figure 1 shows XRR results from a sample grown thermally from oil with chloroform. A simulation is shown offset downward from the data; the parameters providing a simulation most consistent with the data included a film thickness of 1767 Å. XRD revealed crystalline phases attributable to the steel substrate and the oxide but no crystalline tribofilm layers. That result was consistent with the conditions of film creation. Depth-profiled XRF results have not yet been successfully gathered.

Depth-profiled XRD experiments were performed on worn and unworn regions of scuffed SAE 4340 steel. These experiments provided the novel observation of

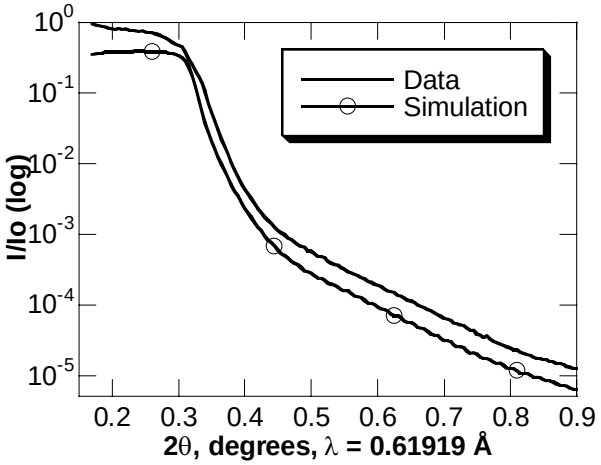

FIG. 1. XRR data and simulation (offset downward) from a tribofilm grown by baking the sample in a chloroform-containing oil.

large volume fractions of the austenite (fcc) phase in worn regions of the normally ferritic (bcc) material [5]. Figure 2 shows the austenite fraction found in the ferrite matrix for worn areas of the samples, for penetration depths of 1.6 and 5.0 μm. No trends were observed in the variation of austenite fraction with tempering temperature. No austenite was detected in unworn regions, except for Group 1, where the austenite fraction was 0.03. The austenite fraction remained the same or decreased slightly from penetration depths of 1.6 to 5.0 μm, indicating that the austenite-containing volume was on the order of 5-μm thick.

In addition to the austenite fraction, the depth-profiled XRD experiments provided information on the dislocation density for future comparison to predictions from adiabatic shear instability theory. The rms strain and domain size were calculated from XRD peak width analysis described by Langford [6]. Dislocation densities were calculated from size and strain results as described by Williamson and Smallman [7]. Figure 3 shows the dislocation density for Group 2 specimens at four stages, from unworn (ground) to fully scuffed. Dislocation densities were the same in unworn areas, in a worn area interrupted before scuffing, and in an area interrupted during scuffing, but they were higher after scuffing.

Discussion

Austenite may have formed in the worn areas as a result of rapid heating to approximately 800°C ("rapid austenitization"), mechanical dissolution of carbides [8], or possibly diffusionless transformation (essentially the reverse of the martensitic transformation) [9]. Since scuffing is observed in many materials that do not display

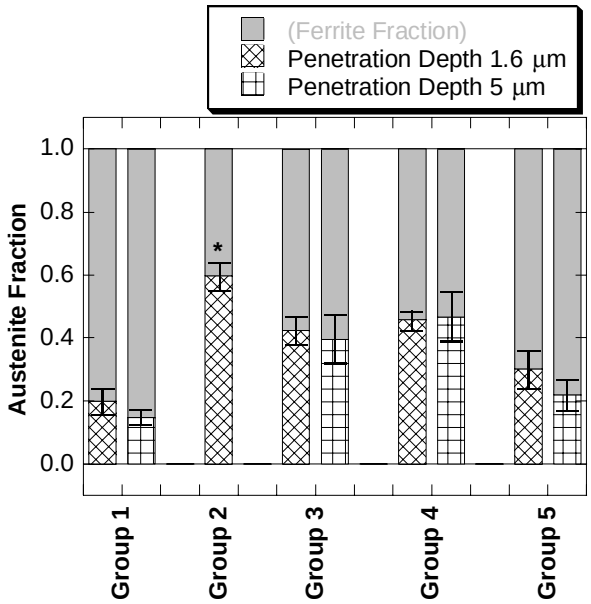

FIG. 2. Austenite and ferrite fractions after scuffing. Results from penetration depths of 1.6 μm are given with a diagonal pattern (except [*] Group 2, where the penetration depth was 1.2 μm). Results from penetration depths of 5 μm are given with a horizontal pattern.

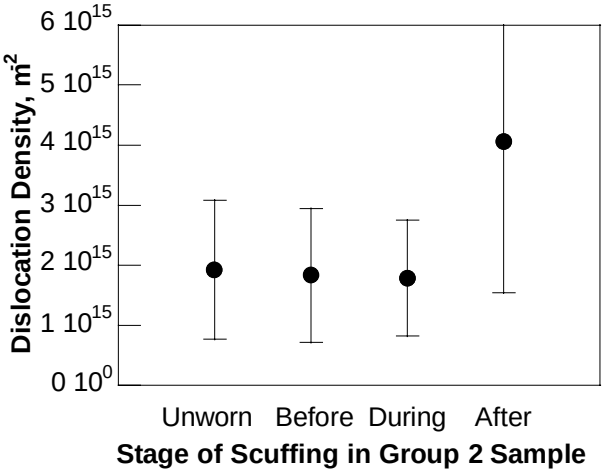

FIG. 3. Dislocation density for four stages of wear in the Group 2 samples.

a phase transformation, scuffing probably occurred before the formation of austenite, not after. However, the formation of austenite may have provided an early initiation mechanism for scuffing in these samples. After formation, the austenite may have been stabilized by stress or by small crystallite size but not likely by compositional change.

The dislocation density results indicate that in the scuffed volumes of the sample interrupted during scuffing, the dislocation density was lower than it was in the completely scuffed sample. This increase in dislocation density after initial scuffing was probably a result of the mechanical deformation caused by severe wear and abrasion by debris, as follows. The initiation of scuffing was associated with heating due to the release of the strain energy of dislocations. This temporary drop in dislocation density was then followed by a rise due to the rapid work of plasticity in the final stages of the wear test, after scuffing initiation. Comparison of the dislocation density values to theory is in progress [10].

Acknowledgments

Use of the APS was supported by the U.S. Department of Energy, Office of Science, Office of Basic Energy Sciences, under Contract No. W-31-109-ENG-38. This project was supported by the BESSR-CAT as an independent investigation. The authors wish to thank J. Zhang and H. Yoon of Caterpillar, Inc., for sample preparation and mechanical testing and H. You of the Materials Science Division at Argonne National Laboratory for assistance on the beamline.

References

[1] J. Enthoven and H. A. Spikes, Trib. Trans. **39**, 441-447 (1996).
[2] K. C. Ludema, Wear **100**, 315-331 (1984).
[3] S. Bec, A. Tonck, J. M. Georges, R. C. Coy, J. C. Bell, and G. W. Roper, Proc. R. Soc. London A **455**, 4181-4203 (1999).
[4] L. G. Parratt, Phys. **95**(2), 359 (1954).
[5] J. Hershberger, O. O. Ajayi, J. Zhang, H. Yoon, and G. R. Fenske, "Formation of austenite during scuffing failure of SAE 4340 steel," Wear (to be submitted, 2002).
[6] J. I. Langford, NIST Special Publication 846 (1992).
[7] G. K. Williamson and R. E. Smallman, Phil. Mag. **1**, 669-683 (1957).
[8] W. Lojkowski, M. Djahanbakhsh, G. Burkle, S. Gierlotka, W. Zielinski, and H. J. Fecht, Mat. Sci. Eng. A **303**, 197-208 (2001).
[9] V. M. Schastlivtsev, I. L. Yaskovleva, T. I. Tabatchikova, and D. A. Mirzaev, J. de Physique IV, Colloque C8 **5**, 531-536 (1995).
[10] J. Hershberger, O. O. Ajayi, J. Zhang, H. Yoon, and G. R. Fenske, "Initiation of Scuffing by Adiabatic Shear Instability, Wear (to be submitted, 2002).